

On the Study of an Autonavagation System for Discharge-Type Microtunneling Machines

Koichi Yoshida * Takeshi Tsujimura*

【Abstract】 On the operation for discharge-type microtunneling machines equipped with laser target positioning system, how to perform direction control of the driving machine based on the obtained sensing data largely depends upon the skill of operators. In this paper, a direction control model which represents the dynamic behavior of the driving machine for head angle control is introduced and an on-line estimation method is adopted to estimate the posture of the driving machine and the model parameters matching the soil condition of the ground, for which direct observation is almost impossible. The direction control model to predict the behavior of the driving machine makes it possible to give an optimal control of the head angle. A prototype of auto navigation system with machine state estimator and optimal direction controller is designed and experimentally applied to an actual construction site, and validity of the navigation system to maintain sound control performance is confirmed.

【Keywords】 Microtunneling, Acemole, Automatic control, Kalman filter, Optimal control

1 Introduction

The microtunneling technology is receiving attention as an alternative method to the open-cut method from the aspects of economy and environmental conditions, and there are demands to increase its range of application and accuracy. Representative microtunneling technologies include the press-insertion method, auger method and balance method. These are selected according to the line shape and the type of soil in the section to be tunneled, as well as economy, low pollution, and so on. The Acemole DL method, which is a kind of slurry and earth pressure balance method, can be used with a variety of excavation cutter heads, enabling it to cope with a wide range of soil, from ordinary soil to ground containing pebbles and rubble stones, and can also be used for tunneling over long distances [1][2]. In addition, new operation systems aimed at reducing the cost for initial installation of foundation facilities have been developed [3]. This paper describes an autonomous navigation system intended for highly accurate, automatic direction control of a discharge-type micro-tunneling machine (Acemole DL method). Previously, the performance of this type of tunneling machine was greatly dependent upon the skill of the operator. This system employs a state transition model that indicates the motion characteristics with respect to direction correction operation of the driving machine. It thus realizes a state estimation function for estimating the overall position and attitude, which are difficult to observe directly, and also a direction correction support function that uses optimal feedback control based on this model. Here, a description is given of the method of configuring a machine state transition model, the method of estimating machine state using a Kalman filter and the method of designing an optimal direction correction control sys-

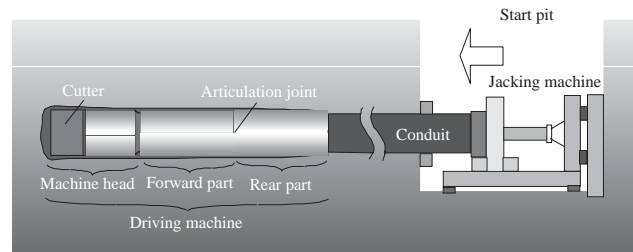


Fig.1: Configuration of discharge-type micro-tunneling machine

tem. The construction of the auto navigation system is also described, and the effectiveness of the system is verified based on the results of evaluating it in on-site tunneling tests.

2 Tunneling Machine Sensing System

Fig.1 shows the overall configuration of the micro-tunneling machine that is intended to be controlled by this system. The cutter at the end of the driving machine advances under the propulsion force of the jacking machine while excavating the ground in the vicinity. The pipeline is formed by adding conduits of constant length one after another. The tunneling direction of the machine can be controlled by inclining the machine head up, down left or right by means of built-in hydraulic jacks.

Fig.2 shows the sensing system, which employs a laser target method, in the case of straight-line tunneling. When the laser beam emitted by the laser theodolite illuminates the target surface of the laser receiving device at the rear of the driving machine, the displacement of the laser receiving device from the reference line (laser beam) can be obtained. On the other hand, the tilt an-

*NTT Access Network Service Systems Laboratories (1-7-1 Hanabatake, Tsukuba-city, Ibaraki, 305-0805)

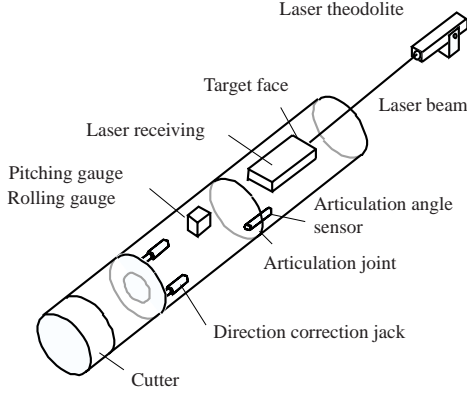


Fig.2: Position detection system employing laser target method

gles in the horizontal and vertical directions with respect to the laser beam at the rear of the driving machine can not be obtained directly, so the each tilt angle is approximated from the change between the displacement of the laser receiving device with respect to the reference line (laser beam) and that measured after the machine has advanced several tens of cm. However, this is based on the assumption that the driving machine does not turn during this interval, so the resulting values are not necessarily accurate. The approximate horizontal and vertical displacements of the articulation joint are obtained from these tilt values. Also, the value obtained from the articulation angle sensor, which detects the relative angle between the front and rear of the driving machine in the horizontal direction, is used to obtain the horizontal position of the machine head, and the pitching gauge installed at the front of the driving machine is used to obtain its vertical position. **Fig.3** shows the horizontal position detection system employing an electromagnetic method, and also the vertical position detection system employing a liquid pressure difference method, which are used to perform curved tunneling. For the horizontal direction, the induction field generated by the sending coil in the driving machine is detected by a magnetic field detecting device on the ground, enabling the horizontal displacement from the projected line to be obtained. For the vertical direction, a pressure sensor in the driving machine detects the difference in the pressure at the point being excavated and the reference liquid pressure, enabling the depth to be obtained.

3 Machine State transition Model

Fig.4 shows the definition of position and angle of each part of the tunneling machine for expressing the state transition model of the machine. The horizontal displacement of the cutter tip as seen from the projected line is X_c , the displacement of the machine head is X_h , the displacement of the articulation joint is X_m , and the displacement of the laser receiving part is X_t . Also, the tilt angle (yawing angle) at the front of the driving

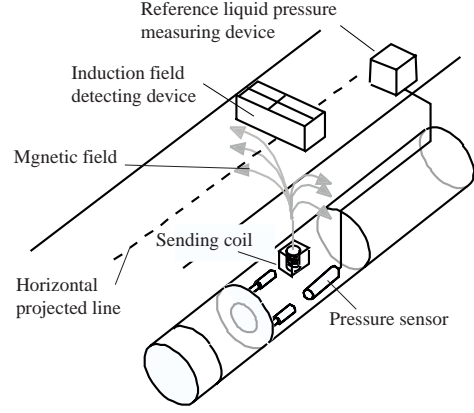


Fig.3: Position detection system employing an induction field detection method and also a liquid pressure detection method

machine with respect to the projected line is θ_H , the tilt angle at the rear of the driving machine is θ_{Hr} , the tilt angle (head angle) at the machine head when the front of the driving machine is taken as a reference is η_H , and the relative angle between front and rear of the driving machine is ϕ (articulation angle). Also, a similar coordinate system can be defined for the vertical direction in order to derive the state transition model, however the description here is limited to the horizontal direction.

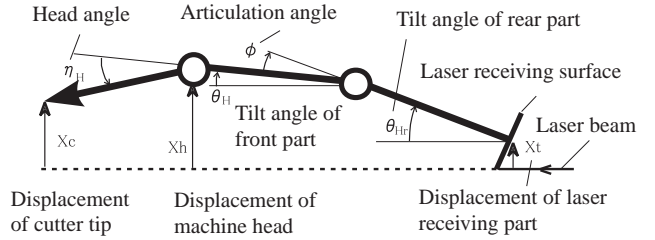


Fig.4: Coordinate system of state transition model

Fig.5 shows the state transition model of the driving machine during unit tunneling length when direction correction motion is performed.

(a) shows the condition when the head angle is changed from η_H by exactly $\Delta\eta_H$ ($\eta'_H = \eta_H + \Delta\eta_H$). Here, if there is no reaction from the ground in the vicinity of the machine, the front edge of the machine will change by exactly $\Delta X_H = L_h \Delta\eta_H$ when the length of the machine head is L_h . However, in actual fact, it is conceivable that there will be a reaction from the ground as indicated by (b), so the following assumption is made for the state transition model.

- < Assumption 1 > A certain proportion, k_{encH} of the displacement ΔX_H of the front edge of the machine due to the head angle change $\Delta\eta_H$ cuts into the ground side. Also, the yawing angle θ_H of the front of the driving machine and the articulation angle ϕ vary with the magnitude of k_{encH} .

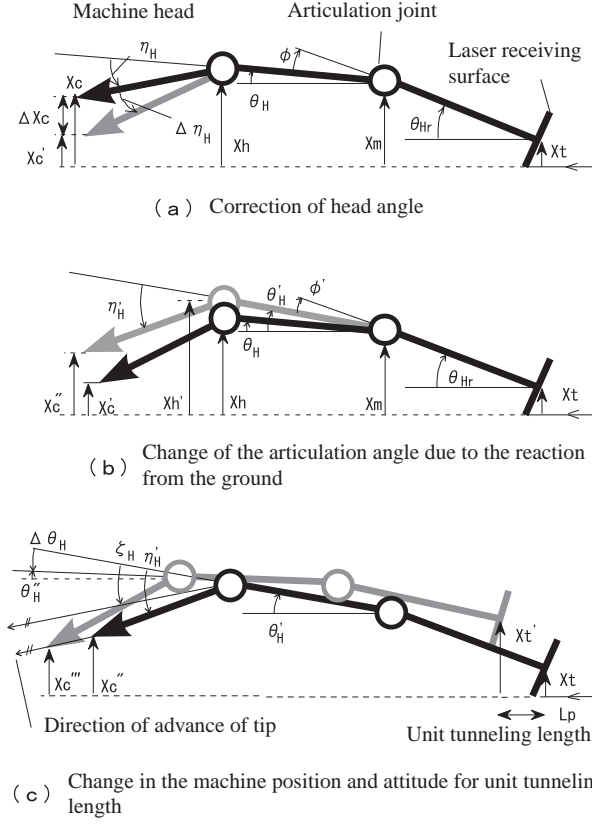


Fig.5: State transition model for unit tunneling length

Here, the front edge X_c'' of the machine after the reaction from the ground shown in **Fig.5** (b) has been taken into account, and the yawing angle θ_H' of the front of the driving machine can be expressed as follows. Note that a downward displacement (right side with respect to the direction of advance) is positive.

$$X_c'' = X_c + k_{encH} L_h \Delta \eta_H \quad (1)$$

$$\theta_H' = \theta_H - \frac{L_h}{L_h + L_f} k_{encH} \Delta \eta_H \quad (2)$$

In these equations, L_f indicates the length of the front of the driving machine. **Fig.5** (c) shows the state transition model when the machine advanced through unit tunneling distance of exactly L_p from the state that it was in after it was subjected to the ground reaction of (b). Here, the following assumptions are made.

< Assumption 2 > The front edge of the machine moved in the direction to which it tilted by an angle of exactly ζ_H with respect to the front of the driving machine. Also, ζ_H is equal to η_H' multiplied by a fixed coefficient $k_{\eta H}$ provided that the characteristics of the soil in the vicinity of the machine do not change.

< Assumption 3 > The change of attitude of the machine per unit tunneling length ($\Delta \theta_H = \theta_H'' - \theta_H'$) is assigned by the linear sum of a limited number of past head angles, including the current head angle,

and the disturbance factor (bias component) that is unrelated to the direction correction operation. Also, the coefficient that expresses the magnitude of the effect on the attitude change for each head angle is constant provided that the characteristics of the soil in the vicinity of the machine do not change.

The above two assumption are expressed by the following two equations.

$$X_c''' = X_c'' + (\theta_H' + k_{\eta H} \eta_H') L_p \quad (3)$$

$$\theta_H'' = \theta_H' + \tilde{b}_0 \eta_H^{(1)} + \tilde{b}_1 \eta_H^{(0)} + \tilde{b}_2 \eta_H^{(-1)} + \dots + \tilde{b}_{nb} \eta_H^{(-nb+1)} + d_H \quad (4)$$

Here, $\eta_H^{(1)} = \eta_H'$, $\eta_H^{(0)} = \eta_H$, and $\eta_H^{(-i)}$ expresses the head angle at a point exactly $i \times L_p$ (m) to the rear of the current position. \tilde{b}_i is a coefficient that expresses the degree to which $\eta_H^{(i)}$ affects $\Delta \theta_H$, and d_H indicates the disturbance factor. Here, if the machine front edge position and also the head angle and yawing angle of the front of the driving machine are expressed as $X_c[k]$, $\theta_H[k]$ and $\eta_H[k]$, respectively, and also the values after the machine has advanced through the unit tunneling distance of (c) are expressed in the form $X_c[k+1](= X_c''')$, $\eta_H[k+1](= \eta_H^{(1)})$, and $\theta_H[k+1](= \theta_H'')$, a state transition model expressed by the following equations is obtained

$$\begin{aligned} X_c[k+1] &= X_c[k] + k_{encH} L_h \Delta \eta_H \\ &+ \left(\theta_H[k] - \frac{L_h}{L_h + L_f} k_{encH} \Delta \eta_H + k_{\eta H} \eta_H[k+1] \right) L_p \\ &= X_c[k] + L_p \theta_H[k] \\ &+ k_{encH} L_h \left(1 - \frac{L_p}{L_h + L_f} \right) \Delta \eta_H + k_{\eta H} L_p \eta_H[k+1] \end{aligned} \quad (5)$$

$$\begin{aligned} \theta_H[k+1] &= \theta_H[k] + \sum_{i=0}^{nb-1} \tilde{b}_i \eta_H[k+1-i] \\ &- \frac{L_h}{L_h + L_f} k_{encH} \Delta \eta_H + d_H \\ &= \theta_H[k] + \left(\tilde{b}_0 - \frac{L_h k_{encH}}{L_h + L_f} \right) \eta_H[k+1] \\ &+ \left(\tilde{b}_1 + \frac{L_h k_{encH}}{L_h + L_f} \right) \eta_H[k] + \sum_{i=2}^{nb-1} \tilde{b}_i \eta_H[k+1-i] + d_H \\ &= \theta_H[k] + \sum_{i=0}^{nb-1} b_{Hi} \eta_H[k+1-i] + d_H \end{aligned} \quad (6)$$

b_{Hi} in the last line of Eq.(6) is the same as each coefficient of $\eta_H[k+1-i]$ in the second line after it has been rewritten.

The following assumption is made concerning the behavior of the rear of the driving machine.

< Assumption 4 > The tilt angle at the rear of the driving machine with respect to the projected line follows the angle at the front of the driving machine with a delay of exactly L_f (m).

Assuming here that the first decimal place of L_f/L_p rounded off to the nearest integer is nd , the above assumption can be expressed by the following equation

$$\theta_{Hr}[k] = \theta_H[k - nd] \quad (7)$$

Concerning the horizontal motion used in the case of straight-line tunneling, it is possible to measure the horizontal position X_t of the laser light receiving surface and also the relative angle between the front and rear of the driving machine (articulation angle ϕ). As shown in **Fig.5**, these can be expressed by the following equations

$$X_t = X_c - L_h(\theta_H + \eta_H) - L_f\theta_H - L_r\theta_{Hr} \quad (8)$$

$$\phi = \theta_H - \theta_{Hr} \quad (9)$$

Where, L_r is the length of the rear of the driving machine.

4 Design of State Estimator

It is not possible to directly measure the values of the variables of the above state transition model such as the horizontal displacement X_c of the front edge of the head and the tilt angle θ_H with respect to the projected line, and it is necessary to estimate them as well as the coefficient b_{Hi} in Eq.(6). A state estimation of these unknown variables is performed using a Kalman filter, based on the state transition model of Eq.(6) and Eq.(5).

4.1 System State Equation Expression

First, the following variable vector $\mathbf{X}_H \in \mathbf{R}^{(nd+2+nb+3) \times 1}$ to be estimated is defined.

$$\mathbf{X}_H[k] \equiv \begin{bmatrix} \theta_H[k] & \theta_H[k-1] & \cdots & \theta_H[k-nd] & X_c[k] \\ b_{H0} & b_{H1} & \cdots & b_{Hnb-1} & d_H & k_{encH} & k_{\eta H} \end{bmatrix}^T$$

Here, it is possible to express Eq.(5) and Eq.(6) by means of the following state equation.

$$\mathbf{X}_H[k+1] = \mathbf{F}_H[k]\mathbf{X}_H[k] + \boldsymbol{\omega}_H[k] \quad (10)$$

Where

$$\mathbf{F}_H[k] = \begin{bmatrix} 1 & \mathbf{O}_{1 \times nd} & 0 & L_p \mathbf{h}_H[k] \\ & \mathbf{I}_{nd} & \mathbf{O}_{nd \times 2} & \mathbf{O}_{nd \times nb} \\ L_p & \mathbf{O}_{1 \times nd} & 1 & \mathbf{O}_{1 \times nb} \\ \hline & \mathbf{O}_{nb \times (nd+2)} & & \mathbf{I}_{nb} \\ & \mathbf{O}_{3 \times (nd+2)} & & \mathbf{O}_{3 \times nb} \end{bmatrix} * \begin{bmatrix} 1 & 0 & 0 \\ & \mathbf{O}_{nd \times 3} \\ 0 & L'_h \Delta \eta_H[k] & L_p \eta_H[k+1] \\ \hline & \mathbf{O}_{nb \times 3} \\ & \mathbf{I}_3 \end{bmatrix}$$

$$\mathbf{h}_H[k] = L_p[\eta_H[k+1] \quad \cdots \quad \eta_H[k-nb+2]]$$

Also, $L'_h = (1 - L_p/(L_h + L_f))L_h$ and $\mathbf{O}_{i \times j}$ and \mathbf{I}_k indicate a zero matrix consisting of i rows and j columns, and also a k -dimensional unit matrix. $\boldsymbol{\omega}_H[k]$ is the system noise consisting of $E(\boldsymbol{\omega}_H) = 0$ and $E(\boldsymbol{\omega}_H[k]\boldsymbol{\omega}_H^T[k']) = \boldsymbol{\Sigma}_{\boldsymbol{\omega}_H} \delta_{kk'}$, $E(\cdot)$ is the expected value, and $\delta_{kk'}$ is Kronecker's delta.

4.2 Observation Equation Using the Laser Method

In this case, the observable signals are laser position X_t and articulation angle ϕ . These signals can be expressed using the following observation equation by using Eq.(8),Eq.(9) and Eq.(7).

$$\mathbf{y}_{HL}[k] = \mathbf{H}_H \mathbf{X}_H[k] + \mathbf{v}_{HL}[k] \quad (11)$$

Where

$$\mathbf{y}_{HL}[k] = \begin{bmatrix} X_t[k] + L_h \eta_H[k] \\ \phi[k] \end{bmatrix}$$

$\mathbf{H}_{HL} = \begin{bmatrix} -L_h - L_f & \mathbf{O}_{1 \times nd} & -L_r & 1 & \mathbf{O}_{1 \times (nb+3)} \\ 1 & \mathbf{O}_{1 \times nd} & -1 & 0 & \mathbf{O}_{1 \times (nb+3)} \end{bmatrix}$ $\mathbf{v}_{HL}[k]$ is the observation noise consisting of $E(\mathbf{v}_{HL}) = 0$ and $E(\mathbf{v}_{HL}[k]\mathbf{v}_{HL}^T[k']) = \boldsymbol{\Sigma}_{\mathbf{v}_{HL}} \delta_{kk'}$.

4.3 Observation Equation Using the Electro-magnetic Method

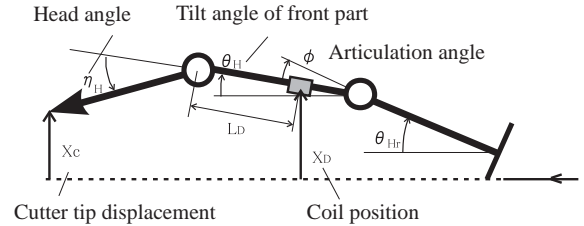


Fig.6: Coordinate system of state transition model

In the electromagnetic method, the magnetic field generated by the sending coil in the driving machine is detected by the magnetic field detector on the ground, enabling the horizontal position of the machine to be detected. As shown in **Fig.6**, this method measures the displacement X_D (coil position) from the projected line. The following equation holds as the observation equation related to the coil position

$$X_D = X_c - L_h(\eta_H + \theta_H) - L_D\theta_H \quad (12)$$

As a rough guide, coil position detection using the induction field detector is performed at an interval of the conduit length. Depending upon the situation at the site, however, measurement may also be performed at odd intervals. Consequently, the observation equation differs according to whether or not coil position detection is performed. The observation equation when the coil position is measured is as follows.

$$\mathbf{y}_{HD}[k] = \mathbf{H}_{HD} \mathbf{X}_H[k] + \mathbf{v}_{HD}[k] \quad (13)$$

Where

$$\mathbf{y}_{HD}[k] = \begin{bmatrix} y_D[k] \\ y_\phi[k] \end{bmatrix} = \begin{bmatrix} X_D[k] + L_h \eta_H[k] \\ \phi[k] \end{bmatrix}$$

$$\mathbf{H}_{HD} = \begin{bmatrix} \mathbf{H}_D \\ \mathbf{H}_\phi \end{bmatrix} = \begin{bmatrix} -L_h - L_D & \mathbf{O}_{1 \times nd} & 0 & 1 & \mathbf{O}_{1 \times (nb+3)} \\ 1 & \mathbf{O}_{1 \times nd} & -1 & 0 & \mathbf{O}_{1 \times (nb+3)} \end{bmatrix}$$

$$\mathbf{v}_{HD} = [v_D \quad v_\phi]^T$$

$$\begin{aligned}
\mathbf{A}' &= \mathbf{T}\mathbf{A}_H\mathbf{T}^{-1} \\
\mathbf{B}' &= \mathbf{T}\mathbf{B}_H \\
\mathbf{C}' &= [\mathbf{O}_{1 \times (nd+1)} \quad 1 \quad \mathbf{O}_{1 \times (nb-1)}] \\
\mathbf{d}' &= \mathbf{T}\mathbf{d}_H
\end{aligned}$$

Here, if d_H is sufficiently small, it is possible to obtain $\mathbf{x}' \rightarrow 0$ and realize $X_t \rightarrow 0$ by performing state feedback control according to the following equation.

$$\nu_H[k] = -\mathbf{K}\mathbf{x}'[k] = -\mathbf{K}\mathbf{T}\mathbf{x}_H[k] \quad (25)$$

By selecting the following evaluation function J , for example,

$$\begin{aligned}
J &= \sum_{k=0}^{\infty} q_{X_t} X_t^2[k] + \nu_H^2[k] \\
&= \sum_{k=0}^{\infty} q_{X_t} \mathbf{x}'^T[k] \mathbf{C}'^T \mathbf{C}' \mathbf{x}'[k] + \nu_H^2[k] \quad (26)
\end{aligned}$$

it is possible to determine the feedback gain \mathbf{K} as follows, by using LQR control logic that optimizes J [6].

$$\mathbf{K} = \left(1 + \mathbf{B}'^T \mathbf{P} \mathbf{B}'\right)^{-1} \mathbf{B}'^T \mathbf{P} \mathbf{A}' \quad (27)$$

Where, \mathbf{P} is the solution to the following Riccati equation.

$$\begin{aligned}
\mathbf{P} &= q_{X_t} \mathbf{C}'^T \mathbf{C}' + \mathbf{A}'^T \mathbf{P} \mathbf{A}' \\
&- \mathbf{A}'^T \mathbf{P} \mathbf{B}' \left(1 + \mathbf{B}'^T \mathbf{P} \mathbf{B}'\right)^{-1} \mathbf{B}'^T \mathbf{P} \mathbf{A}' \quad (28)
\end{aligned}$$

Here, q_{X_t} indicates the weighting concerning the convergence of X_t . The larger this value, the faster is the convergence (response) to 0.

6 Direction Correction Control Test

Below are described the results of performing an on-site tunneling test using a prototype auto navigation system that employs the abovementioned state estimation and direction correction control methods.

6.1 Auto Navigation System

The various kinds of sensor data from the driving machine are transferred sequentially into the operation panel by the sequencer, and enter the navigation PC via the add-on link unit. The data analysis results and direction correction control instruction values are displayed on, and each parameter is set from, the externally installed LCD panel via the user interface software. The optimal direction correction provided by the system is assigned by the operator by operating the machine head tilting hydraulic jack. **Fig.7** shows an example of operation of the software used in the implementation test. On the left and right sides of the screen are displayed data concerning the horizontal and vertical directions, respectively. The horizontal axis of both graphs indicates the relative tunneling distance, and 0 m indicates

the present position. To the left of this point the observation results obtained so far are displayed, and to the right of it the predicted response based on a simulation of the case where optimal direction correction control is performed from now on is displayed. The upper graph indicates the head angle input. The bar graph on the negative side of the horizontal axis (past data) indicates the head angle actually assigned to the machine by the operator, and the mark indicates the optimal head angle input computed by the navigation system. The lower graph indicates the displacement of the laser target, and the thick line on the negative side of the horizontal axis indicates the data obtained from actual observation. The thin line indicates the predicted laser target displacement at a certain point, based on the state transition model estimated at a point about 2 m in the past from the above point. A comparison with the thick line provides a rough indication for evaluating the suitability of the estimated state transition model. Also, when using the electromagnetic method, the display changes over to a graph display of the coil position [4].

6.2 Tunneling Test Results

An on-site tunneling test for direction correction control was performed using the Acemole DL50. Table 1 shows the external dimensions and other specifications of the machine pertaining to navigation.

Table 1 Specifications of DL50 driving machine

External dimensions		$\phi 457 \times 3257$ mm
Weight		2198 kgf
Direction correction jack		12t \times 20st \times 3
Machine head	L_h	1000 mm
Front of driving machine	L_f	1117 mm
Rear of driving machine	L_r	1144 mm
Sending coil position		L_D 745 mm

The unit tunneling length over which the tunneling data is sampled (except coil position detection) was $L_p = 0.1$ m. Consequently, the selected order related to the delay at the rear of the driving machine introduced in < Assumption 4 > is $nd = 11$. Also, regarding < Assumption 3 >, nb was assumed to be equal to 5 in Eq.(6).

Fig.8 shows the results of evaluating direction correction control in a section where tunneling is performed in a straight using the laser target method. Like the display of **Fig.7**, the mark in the graph that indicates the horizontal head angle η_H indicates the optimal head angle input computed by the system, and the bar graph indicates the actual head angle input assigned by the operator. Also, the thick line in the graph that indicates the horizontal displacement X_t of the laser target indicates the observed value, and the thin line is a plot of the predicted displacement at a certain point, based on the state transition model estimated at a point about 2 m in the past from the above point. Concretely, it is the value obtained by using the state estimation value

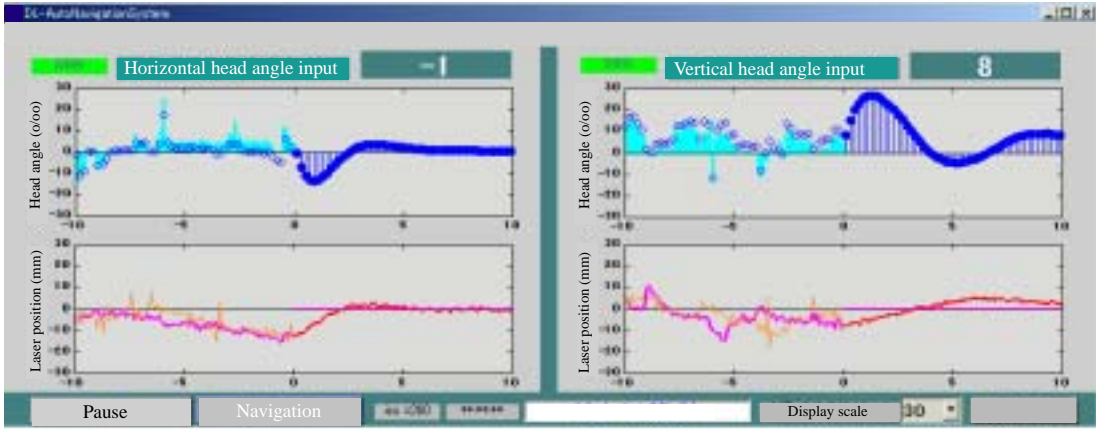


Fig.7: Display examples of user interface software for the auto navigation system

X_H for a point 2 m in the past as the initial value, and then integrating Eq.(21) over a distance of 2 m. Consequently, if there is an error in the initial value, it will be accumulated in the estimated value. The trend of the response of X_t can be seen from the predicted plot, and it can be said that the estimation results obtained are appropriate for a machine state transition model. The actual head angle input differs by several $^{\circ}/_{00}$ with respect to the optimal head angle input provided by the system. This is due to manual operation by the operator, which has limited accuracy because of the characteristics of the machine direction correction jacks. It was confirmed, however, that satisfactory direction correction motion could be maintained over this evaluation section.

The thick line in **Fig.9** indicates the estimated results for the horizontal position and attitude of the driving machine in this section. The thin line indicates the estimated values resulting from data processing using the conventional operation panel. These values were obtained as follows: First, the angle of the driving machine with respect to the reference line at the rear of the driving machine was obtained from the change in the displacement of the laser light receiving part at 60-cm tunneling intervals, and then the articulation angle sensor data was added, enabling the position and attitude of the driving machine to be obtained. As can be seen from the figure, the data processing method, which is based on the difference between the 60-cm intervals, produces a lot of noise. Particularly, large errors occur in the estimated values of position and attitude of the driving machine when discontinuous changes in the laser displacement data appear immediately after the start of pushing, for example. This can be misleading to an inexperienced operator. On the other hand, because the estimated value based on the state transition model is computed based on the construction of the machine, the error dispersion of the sensor data, and so on, it is possible to obtain smoother estimated results.

The estimated values in the evaluation section for each of the parameters in state transition model Eq.(5) and

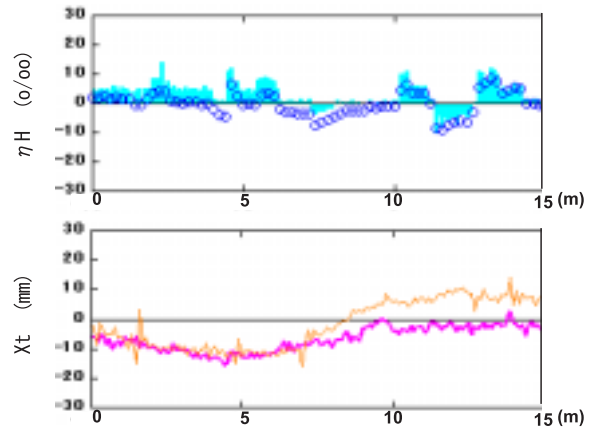


Fig.8: Results of horizontal direction correction control

Eq.(6), and so on, are roughly constant. Table 2 shows the combined values for the horizontal and vertical directions. **Fig.10** shows the results of evaluating vertical direction correction control. Y_t is the vertical displacement of the laser target.

Table 2 Estimated values of the model parameters

b_{H0}	-0.207	b_{V0}	-0.691
b_{H1}	0.199	b_{V1}	0.471
b_{H2}	0.024	b_{V2}	0.295
b_{H3}	-0.032	b_{V3}	-0.04
b_{H4}	0.1	b_{V4}	0.079
k_{encH}	0.9	k_{encV}	0.74
$k_{\eta H}$	0.1	$k_{\eta V}$	0.47

Fig.11 shows the evaluation results for the case where direction correction control was performed using the electromagnetic method, which detects the magnetic field generated by the sending coil inside the driving machine from above the ground. This method was used because the gradient of the vertical projected line changes mid-way thus the laser target method is no longer available after the break point despite the fact that the horizontal projected line is straight. The displacement X_D of the coil with respect to reference line measured using the

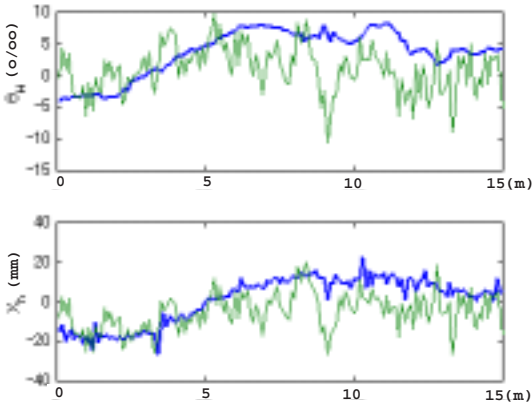


Fig.9: Results of estimating horizontal position and attitude of the driving machine

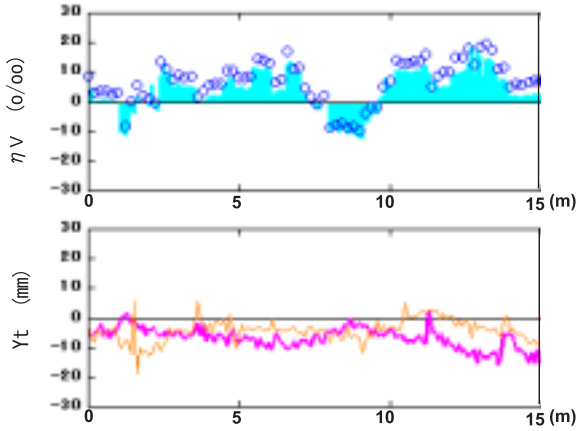


Fig.10: Results of vertical direction correction control

induction field detecting device is indicated by the symbol \bullet . While the position detection by the electromagnetic method is being stopped until the next detection, state estimation is performed only by the articulation angle data to estimate the position of the coil. These estimated position values are indicated by the solid line. From **Fig.11**, the difference between the estimated value prior to coil position detection obtained using the state transition model, and the value measured by the induction field detecting device, is about 10~20 mm. It is thus possible to verify the effectiveness of the state transition model in this evaluation section, and also it can be seen that satisfactory direction correction control operation can be maintained.

In the tunneling section shown in **Fig.11**, the projected line was straight in the horizontal direction, but its gradient changed mid-way in the vertical direction, preventing the laser from being used, so direction correction was performed using the electromagnetic method. If it is necessary to perform curved tunneling, this can be done by rewriting the position and attitude variables of Eq.(10) to a state equation the displacement of which is based on a curve. However, verification by on-site tunneling tests remains a topic for the future.

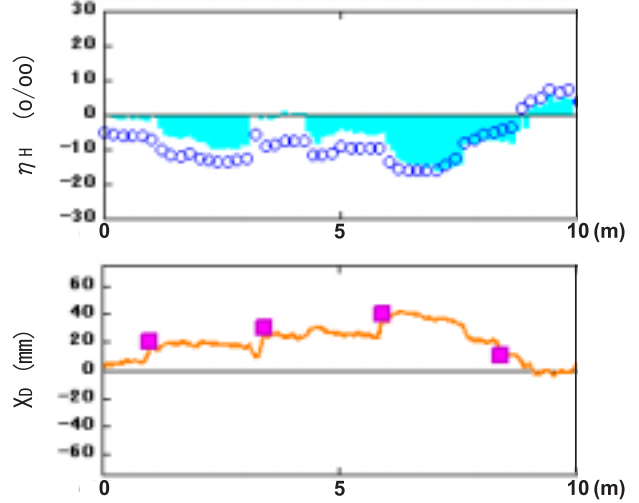


Fig.11: Results of direction correction control when the electromagnetic method is used

7 Conclusion

An auto navigation system aimed at highly accurate automatic direction correction control of a discharge-type micro-tunneling machine was developed. This system uses a state transition model that indicates the motion characteristics of the driving machine with respect to the direction correction operation. It thus realizes a state estimation function for estimating the overall position and attitude of the machine, which are difficult to observe directly, and also a direction correction support function that uses optimal feedback control based on this model. As a result of performing an on-site tunneling test, it was confirmed that satisfactory correction control operation can be maintained in the tunneling evaluation section, using the laser target method and the electromagnetic method.

References

- [1] Yato: Comparison Manual for Selecting Microtunneling Methods, Kindai Tosho, 1998 (in Japanese).
- [2] Microtunneling Method Research Society: Planning and Design of Microtunneling Methods, Economic Research Association, 1997 (in Japanese).
- [3] Awata, Miyatake, Mikawa: Automated Driving Management and Control System Using Knowledge Database and Optimal Control Theory, Proc. of 11th Trenchless Technology Research Presentation Treatises, pp.3-10, 2000 (in Japanese).
- [4] K. Yoshida and T. Tsujimura: Auto Navigation System for Discharge-Type Microtunneling Machine, Proc. of 11th Trenchless Technology Research Presentation Treatises, pp.11-18, 2000 (in Japanese).
- [5] Nakano, Nishiyama: Kalman Filter Design Using a Personal Computer, Maruzen, 1996 (in Japanese).
- [6] Mita, Hara, Kondo: Introduction to Digital Control, Corona Publishing, 1988 (in Japanese).